# Trajectory Planning Method for Multi-USV Cooperative Occupying Based on Dubins Curves

**Wenxuan Sun***
*Jiangsu Automation Research Institute, Lianyungang, Jiangsu, China*
** Corresponding Author*

**Abstract: Aiming at the operational requirement of occupying positions during multi-unmanned surface vehicle (USV) cooperative combat, this paper studies the trajectory planning problem in the multi-USV cooperative occupying phase and proposes a trajectory planning algorithm based on Dubins curves. For the single-USV trajectory solving problem, a discriminant table is used instead of traditional methods to improve the process of calculating six cases in the Dubins curve geometric method, reducing the calculation time. For the time constraints of multi-USV cooperative combat, a time coordination method for occupying trajectories is studied. The coordination arrival time at occupying points is determined based on the navigation time of single-USV occupying trajectories, and the navigation speed of each USV is planned under tangential acceleration and velocity constraints to ensure arrival at the positions at specified times. The proposed trajectory planning algorithm is verified through simulation experiments.**

**Keywords: Unmanned Surface Vehicle (USV); Cooperative Combat; Occupation; Trajectory Planning; Time Coordination**

## 1. Introduction

With the rapid development of unmanned equipment, unmanned surface vehicles (USVs), as frontier forces in unmanned battlefield environments, are playing an increasingly important role in future war forms. Characterized by small size, flexibility, and high speed, multiple USVs can jointly carry out cooperative strikes and saturation attacks on targets [1,2]. Considering that USVs need to occupy their respective positions during cooperative attack missions and maintain certain speeds and headings upon arrival [3], designing occupying trajectories for USVs that meet speed, time, and attitude requirements with high navigability is of great significance for effective cooperative strikes.

Most current path planning methods do not consider performance constraints and often use spatial graph methods such as grid maps [4,5], probabilistic roadmap graphs [6], and Voronoi diagrams [7]. The planning results often contain numerous corners, making the trajectories unnavigable. Although dynamic planning methods can satisfy model performance constraints [8], they have long calculation times and are unsuitable for fast real-time planning scenarios. Dubins curves are the shortest curves from a start state to an end state considering the influence of the turning radius on the moving body’s motion. They solve the curve length geometrically, with solution time independent of the map range, making them suitable for trajectory planning in large-scale battlefield environments [9].

This paper decomposes the cooperative positioning trajectory planning problem into two layers: single-USV trajectory planning and multi-USV trajectory coordination, to generate trajectories meeting the requirements of multi-USV cooperative occupying.

## 2. Fast Trajectory Planning Method for Single USV Occupying

### 2.1 Dubins Model for Unmanned Surface Vehicle

According to the definition of Dubins paths [10]: given the vector directions at two points in space, the shortest path between these points consists of "arc-tangent-arc," "arc-arc-arc," or their subset curves, with the turning radius in the arc segments satisfying the minimum turning radius constraint. Therefore, the pose of a moving body at any moment can be represented by $q = (x, y, \theta)$, where $(x, y)$

 

denotes the coordinate position in space, and $\theta$ denotes the heading angle of the moving body at that position. The shortest path between any two different pose points $D_{min}$ belongs to one of the following six types:

$$D_{min}$$

The shortest curve among these six path types is called the Dubins path. Here, $L$ represents the moving body turning left at the minimum radius, $R$ represents the moving body turning right at the minimum radius, and $S$ represents the moving body moving straight at the current heading. Schematic diagrams of the six Dubins curves are shown in Figure 1, where the starting point is $B(x_0, y_0, \theta_0)$ and the ending point is $E(x_1, y_1, \theta_1)$.

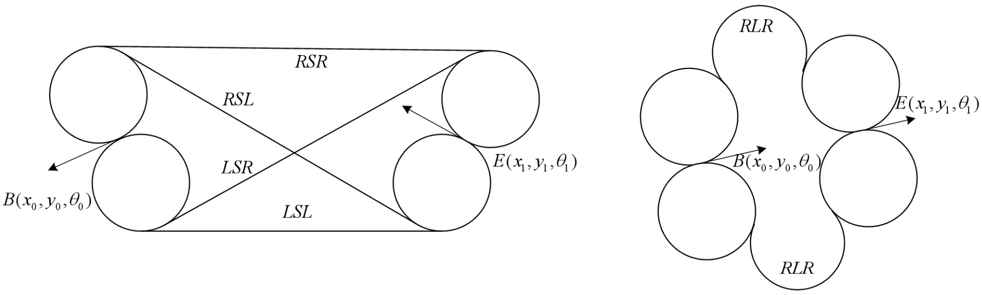


**Figure 1. Schematic Diagram of Six Typical Dubins Paths**

The kinematic equations of the USV are established as:

$$\begin{cases} \dot{x} = v\cos\psi \\ \dot{y} = v\sin\psi \end{cases} \tag{1}$$

Where $x, y$ are the position components of the USV in the horizontal plane, $v$ is the navigation speed, and $\psi$ is the heading angle.

Assuming all USVs are of the same type, their constraint conditions are identical. The following constraints are considered:

Due to the curved nature of the USV's trajectory, which has a maximum curvature constraint, it can be characterized by the minimum turning radius:

$$r(e) \geq r_{min} \tag{2}$$

Where $e$ is an arbitrary point on the path, and $r_{min}$ is the minimum turning radius of the USV. The minimum turning radius constraint of the USV is related to the centripetal acceleration constraint along the path.

The tangential acceleration at any point on the USV's path must be less than the maximum tangential acceleration, expressed as:

$$|a| \leq a_{max} \tag{3}$$

where $a_{max}$ denotes the maximum available tangential acceleration of the USV.

Additionally, the USV's velocity constraint must be satisfied:

$$vmax_{min} \tag{4}$$

where $v_{min}$ and $v_{max}$ are the minimum and maximum velocities of the USV, respectively. The instantaneous velocity of the USV must fall within this interval; otherwise, if the velocity is excessively high or low, the USV cannot accelerate/decelerate to meet the requirements and will fail to navigate along the planned positioning trajectory.

### 2.2 Single-USV Occupying Trajectory Generation

Given the highly dynamic battlefield environment, the traditional method for calculating Dubins curves is improved to enhance the rapidity of positioning trajectory solution, enabling faster trajectory planning for USVs and improving their combat effectiveness. The improvements are as follows: A logical discriminant table [11] is introduced to directly determine the type of the shortest path based on the quadrants of the heading angles at the start and end points of the plan and discriminant functions. This allows obtaining the waypoints of the occupying trajectory in a single step.

The logical discriminant table is shown in Table 1.

To calculate the discriminant parameters in the discriminant table, the following two discriminant functions are required:

$$f(s1, s2, s3) = s1 - s2 - 2(s3 - \pi)$$
$$g(s) = s - \pi \tag{5}$$

The corresponding discriminant parameters can be calculated based on the quadrants of the heading angle in the initial pose and the heading angle in the occupation point pose, and the calculation formula of the discriminant parameters is as follows.

$$S_{12} = f(p_{rsr}, p_{rsl}, q_{rsl})$$
$$S_{13} = g(t_{rsr})$$
$$S_{14}^{1} = g(t_{rsr}),\ S_{14}^{2} = g(q_{rsr})$$
$$S_{21} = f(p_{lsl}, p_{rsl}, t_{rsl})$$
$$\begin{cases} if\ \alpha > \beta, S_{22}^{1} = f(p_{lsl}, p_{rsl}, t_{rsl}) \\ if\ \alpha < \beta, S_{22}^{2} = f(p_{rsr}, p_{rsl}, q_{rsl}) \end{cases}$$
$$S_{24} = g(q_{rsr})$$

$$S_{31} = g(q_{lsl})$$

 

$$\begin{cases} if\ \alpha < \beta, S_{33}^1 = f(p_{rsr}, p_{lsr}, t_{lsr}) \\ if\ \alpha > \beta, S_{33}^2 = f(p_{lsl}, p_{lsr}, q_{lsr}) \end{cases}$$
$$S_{34} = f(p_{rsr}, p_{lsr}, t_{lsr})$$
$$S_{41}^1 = g(t_{lsl}),\quad S_{41}^2 = g(q_{lsl})$$
$$S_{42} = g(t_{lsl}) \tag{6}$$
$$S_{43} = f(p_{lsl}, p_{lsr}, q_{lsr})$$

Using the logical discriminant table, the shortest smooth path between the initial and target pose points can be determined without explicitly computing all types of Dubins curves.

**Table 1. Discriminant Table for Dubins Shortest Path Types**

| Target Heading Quadrant \ Initial Heading Quadrant | 1 | 2 | 3 | 4 |
|---|---|---|---|---|
| 1 | $RSL$ | $if\ S_{12} < 0\ then\ RSR$<br>$if\ S_{12} > 0\ then\ RSL$ | $if\ S_{13} < 0\ then\ RSR$<br>$if\ S_{13} > 0\ then\ LSL$ | $if\ S_{14}^1 > 0\ then\ LSR$<br>$if\ S_{14}^2 > 0\ then\ RSL$<br>$else\quad RSR$ |
| 2 | $if\ S_{21} < 0\ then\ LSL$<br>$if\ S_{21} > 0\ then\ RSL$ | $if\ S_{22}^1 < 0\ then\ LSL$<br>$if\ S_{22}^1 > 0\ then\ RSL$<br>$if\ S_{22}^2 < 0\ then\ RSR$<br>$if\ S_{22}^2 > 0\ then\ RSL$ | $RSR$ | $if\ S_{24} < 0\ then\ RSR$<br>$if\ S_{24} > 0\ then\ RSL$ |
| 3 | $if\ S_{31} < 0\ then\ LSL$<br>$if\ S_{31} > 0\ then\ LSR$ | $LSL$ | $if\ S_{33}^1 < 0\ then\ RSR$<br>$if\ S_{33}^1 > 0\ then\ LSR$<br>$if\ S_{33}^2 < 0\ then\ LSL$<br>$if\ S_{33}^2 > 0\ then\ LSR$ | $if\ S_{34} < 0\ then\ RSR$<br>$if\ S_{34} > 0\ then\ LSR$ |
| 4 | $if\ S_{41}^1 > 0\ then\ RSL$<br>$if\ S_{41}^2 > 0\ then\ LSR$<br>$else\quad LSL$ | $if\ S_{42} < 0\ then\ LSL$<br>$if\ S_{42} > 0\ then\ RSL$ | $if\ S_{43} < 0\ then\ LSL$<br>$if\ S_{43} > 0\ then\ LSR$ | $LSR$ |

## 3. Multi-USV Occupying Trajectory Time Coordination Algorithm

After planning the occupying trajectory for each individual USV, a velocity coordination method is employed to incorporate the USV's velocity performance constraints into the trajectory time coordination process. This ensures that multiple USVs can arrive at their respective positions simultaneously, enabling multi-directional cooperative attacks on the target.

### 3.1 Time Planning for Occupying Trajectories

Using the single-USV occupying trajectory planning method, for each USV executing the same strike mission, given the initial pose $P_{p,i}(x_{p,i}, y_{p,i}, \psi_{p,i})$ and the target pose $P_{q,i}(x_{q,i}, y_{q,i}, \psi_{q,i})$, the length of the occupying trajectory can be calculated and denoted as $l_i$

To calculate the minimum navigation time of the USV for a given occupying trajectory length, it is first necessary to compute two reference lengths, denoted as $l_{i,1}$, $l_{i,2}$. Here, $l_{i,1}$ represents the distance traveled by the $i$-th USV during the process of accelerating from its initial pose to the maximum speed and then changing from the maximum speed to the formation cruising speed, while $l_{i,2}$ represents the distance traveled by the $i$-th USV when navigating from the initial pose to the formation cruising speed at the maximum tangential acceleration. The calculation formulas are as follows:

$$\begin{aligned} l_{i,1} &= \frac{v_{\max}^2 - v_{p,i}^2}{2a_{\max}} + \frac{v_{\max}^2 - v_{q,i}^2}{2a_{\max}} \\ l_{i,2} &= \frac{\left|v_{q,i}^2 - v_{p,i}^2\right|}{2a_{\max}} \end{aligned} \tag{7}$$

Based on the magnitude relationship between the occupied trajectory length and the reference lengths, it is found that when the occupying trajectory's length is smaller than the smaller value of the reference lengths, the USV cannot navigate along this occupying trajectory due to the tangential acceleration constraint. Therefore, it is necessary to increase the USV turning radius for replanning so that the length of the newly planned occupying trajectory is not less than the smaller value of the reference lengths. In other cases, the minimum navigation time of the USV can be calculated using the following formula:

$$t_{i,\min} = \begin{cases} \dfrac{\sqrt{a_{\max} l_i + \dfrac{v_{p,i}^2 + v_{q,i}^2}{2}} - v_{p,i}}{a_{\max}} + \dfrac{\sqrt{a_{\max} l_i + \dfrac{v_{p,i}^2 + v_{q,i}^2}{2}} - v_{q,i}}{a_{\max}}, & l_{i,1} \ge l_i \ge l_{i,2} \\ \dfrac{v_{\max} - v_{p,i}}{a_{\max}} + \dfrac{v_{\max} - v_{q,i}}{a_{\max}} + \dfrac{l_i - l_{i,1}}{v_{\max}}, & l_i > l_{i,1} \end{cases} \tag{8}$$

Similarly, to determine the maximum navigation time of the USV for a given occupying trajectory length, another reference length, denoted as $l_{i,3}$, needs to be determined. $l_{i,3}$ is the distance traveled by the $i$-th USV during the process of decelerating from the initial pose velocity to the minimum speed at the fastest rate and then changing from the minimum speed to the formation cruising speed. The calculation formula is as follows:

$$l_{i,3} = \frac{v_{p,i}^2 - v_{min}^2}{2a_{max} + \frac{v_{q,i}^2 - v_{min}^2}{2a_{max}}} \tag{9}$$

Therefore, the calculation method for the maximum navigation time of the USV can be expressed by the following formula:

$$t_{i,\max} = \begin{cases} \dfrac{v_{p,i} - \sqrt{a_{\max} l_i + \frac{v_{p,i}^2 + v_{q,i}^2}{2}}}{a_{\max}} + \dfrac{v_{q,i} - \sqrt{a_{\max} l_i + \frac{v_{p,i}^2 + v_{q,i}^2}{2}}}{a_{\max}}, & l_{i,3} \ge l_i \ge l_{i,2} \\ \dfrac{v_{p,i} - v_{\min}}{a_{\max}} + \dfrac{v_{q,i} - v_{\min}}{a_{\max}} + \dfrac{l_i - l_{i,3}}{v_{\min}}, & l_i > l_{i,3} \end{cases} \tag{10}$$

The objective of multi-USV trajectory time coordination is to enable all USVs to arrive at their respective occupation positions simultaneously, while minimizing the arrival time for each USV. Therefore, the maximum value in the set of minimum times required for each USV to navigate along its respective occupied trajectory is taken as the coordinated arrival time at the occupation points, i.e.:

$$T \underset{i=1,\dots,N}{max} i.min_{min} \tag{11}$$

Using this method, the following equation needs to be satisfied:

$$T \underset{i=1,\dots,N}{min} i.max\, max_{min} \tag{12}$$

In the equation, $T_{max}$ represents the minimum value in the set of maximum times required for each USV to navigate along its respective occupying trajectory. If the above equation is not satisfied, the USV turning radius must be increased to ensure $Ti, max_{min}$.

### 3.2 Speed Planning for Occupying Trajectories

After determining the multi-USV coordinated arrival time, it is necessary to plan the navigation speed for each USV to ensure it reaches its occupation position at the desired time. During the planning process, the tangential acceleration constraints and maximum/minimum navigation speed constraints of the USV are considered, as shown in Equations (3) and (4).

According to Equation (12), the minimum time for a USV to reach its occupation position is $T_{min}$. The objective of speed planning is to make the arrival time of each USV at its occupation position equal to $T_{min}$. Known variables in the speed planning process include the initial pose velocity $v_{p,i}$, the formation cruising velocity $v_{q,i}$, the occupying trajectory navigation time $T_{min}$, and the occupying trajectory length $l_i$. Therefore, speed planning must satisfy the following conditions:

$$\begin{cases} \int_0^{T_{min}\int} v_i(t)dt = l_i \\ v_i(0) = v_{p,i} \\ v_i(Tq, i_{min}\{ \end{cases} \tag{13}$$

Additionally, to satisfy the tangential acceleration constraints and velocity constraints of the USV, the speed planning must also meet the following conditions:

$$\begin{cases} v_{\min} \le v_i(t) \le v_{\max} \\ |\dot{v}_i(t)| \le a_{\max} \end{cases} \tag{14}$$

For the rapidity and practicality of speed planning, it is considered that the USV adopts the maximum tangential acceleration for speed planning. Four time-velocity curves can be obtained from Equations (13) and (14), as shown in Figure 2:

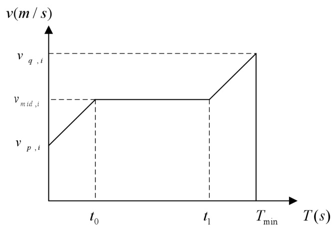


a) $v_{p,i} < l_i/Tq, i_{min}$

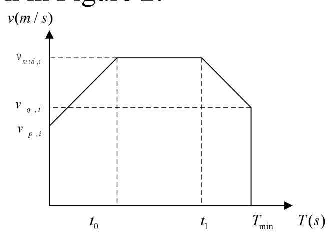


b) $v_{p,i} \le l_i/Tq, i_{min_{min}}$

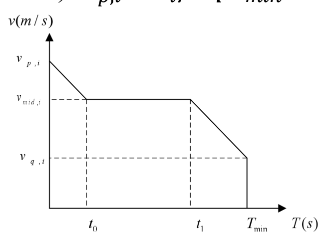


c) $v_{p,i} > l_i/Tq, i_{min}$

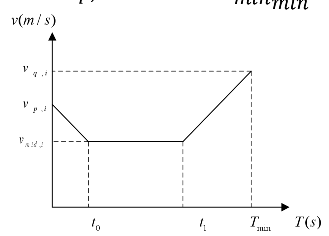


d) $v_{p,i} \ge l_i/Tq, i_{min_{min}}$

**Figure 2. Time-Velocity Curves**

The parameters involved in the above scenarios all satisfy the following system of equations:

$$\begin{cases} \dfrac{v_{mid,i}^2 - v_{p,i}^2}{2a_{\max}} + \dfrac{v_{mid,i}^2 - v_{q,i}^2}{2a_{\max}} + v_{mid,i}(t_1 - t_0) = l_i \\ \dfrac{\left|v_{mid,i} - v_{p,i}\right| + \left|v_{mid,i} - v_{q,i}\right|}{a_{\max}} + t_1 - t_0 = T_{\min} \\ t_0 = \left|\dfrac{v_{mid,i} - v_{p,i}}{a_{\max}}\right| \end{cases} \tag{15}$$

For the above four scenarios, speed adjustment methods are designed respectively.

Scenario 1: $v_{p,i} < l_i/Tq, i_{min}$ or $v_{p,i} > l_i/Tq, i_{min}$

By removing the absolute value from Equation (15), the system of equations for speed planning parameters is obtained as follows:

$$\begin{cases} v_{mid,i} = \dfrac{l_i - \dfrac{v_{q,i}^2 - v_{p,i}^2}{2a_{\max}}}{T_{\min} - \dfrac{v_{q,i} - v_{p,i}}{a_{\max}}} \\ t_0 = \dfrac{v_{mid,i} - v_{p,i}}{a_{\max}} \\ t_1 = T_{\min} - \dfrac{v_{q,i} - v_{mid,i}}{a_{\max}} \end{cases} \tag{16}$$

Scenario 2: $v_{p,i} \le l_i/T_{min}$ and $v_{q,i} \le l_i/T_{min}$, or, $v_{p,i} \ge l_i/T_{min}$ and $v_{q,i} \ge l_i/T_{min}$

Similarly, the system of equations for speed planning parameters can be obtained as follows:

$$\begin{cases} v_{mid,i} = x_{mid,i,2} \\ t_0 = \dfrac{v_{p,i} - v_{q,i}}{a_{max}} \\ t_1 = T\dfrac{v_{q,i} - v_{mid,i}}{a_{max}}\{_{min} \end{cases} \tag{17}$$

In the equation, $x_{mid,i,2}$ is a discriminant parameter, and its calculation formula is as follows:

$$x_{mid,i,2} = \frac{(2a_{\max}T_{\min} + 2v_{p,i} + 2v_{q,i}) - \sqrt{\Delta}}{4}$$
$$\Delta = 4(a_{\max}T_{\min} + v_{p,i} + v_{q,i})^2 - 8(v_{p,i}^2 + v_{q,i}^2 + 2a_{\max}l_i) \tag{18}$$

In summary, after planning the speeds for multiple USVs and obtaining the speed planning parameters, the USVs can navigate along the occupying trajectories at the planned speeds to arrive at the occupation positions simultaneously. The pseudocode for the designed time coordination algorithm is shown in Table 2.

## 4. Case Simulation

A numerical simulation method is used to verify the proposed multi-USV cooperative occupying trajectory planning method. The specific simulation condition settings are shown in Table 3:

**Table 2. Pseudocode for Multi-USV Occupying Trajectory Time Coordination Algorithm**

| Multi-USV Occupying Trajectory Time Coordination Algorithm | |
|---|---|
| 1: | Each USV's occupying trajectory is planned using Dubins curves |
| 2: | for i=1:N do |
| 3: | if (li<li,2) then |
| 4: | Increase the length of the single-USV’s occupying trajectory by increasing the turning radius |
| 5: | end if |
| 6: | Calculate the maximum and minimum times for USVs to navigate along their occupying trajectories |
| 7: | end for |
| 8: | Calculation Tmin |
| 9: | for i=1:N do |
| 10: | if (Tmin>ti,max) then |
| 11: | Increase the time of the single-USV’s occupying trajectory by increasing the turning radius |
| 12: | Update Tmin |
| 13: | end if |
| 14: | end for |
| 15: | for i=1:N do |
| 16: | Generate the velocity planning result for the *i*-th USV. |
| 17: | end |

**Table 3. Simulation Initial Conditions**

| USV Number | Starting Pose | Occupation Pose | Initial Velocity (m/s) | Formation Velocity (m/s) |
|---|---|---|---|---|
| USV1 | (-100, 600,90°) | (200, 300, 0°) | 10 | 20 |
| USV2 | (-100, 0, 90°) | (500, 300, 0°) | 12 | 20 |
| USV3 | (-100, 400, 90°) | (300, 300, 0°) | 18 | 20 |
| USV4 | (-100, 200, 90°) | (400, 300, 0°) | 9 | 20 |

The constraint conditions for USVs are shown in Table 4:

**Table 4. The Constraint Conditions for USVs**

| Constraint term | Parameter value |
|---|---|
| Minimum turning radius | 30m |
| Maximum available speed | 25m/s |
| Minimum available speed | 5m/s |
| Maximum tangential acceleration | 5m/s2 |

The heading angle variation curves of each USV along the occupying trajectory are shown in Figure 3.

As can be seen from the figure, the heading changes along the occupying trajectory are smooth, with the heading angle varying within the range of [0, 360°]. The planned occupying trajectory connects the starting position to the target position, and the heading at the trajectory endpoint matches the heading required by the occupation pose.

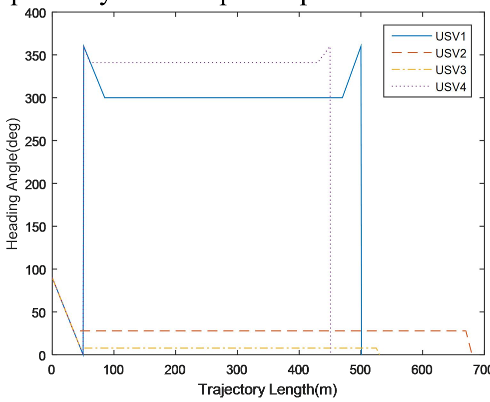


**Figure 3. Heading Angle Variation Curves**

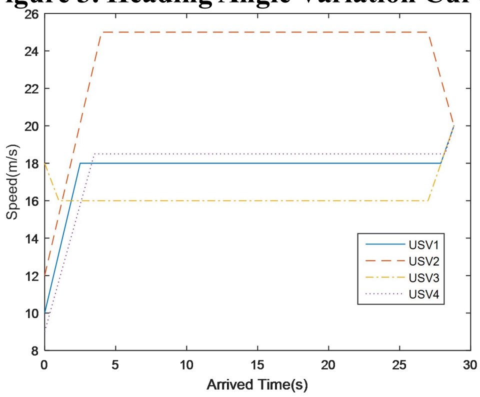


**Figure 4. Time-Velocity Curves of Each USV**

Using Equations (9) and (11), we can calculate $t_{i,min}$ and $t_{i,max}$, thus obtaining $T_{min}$ and $T_{max}$. Therefore, the time for all USVs to reach their occupation positions simultaneously is determined to be 28.82 seconds. The velocity variation curves along the occupying trajectory are shown in Figure 4. It can be seen that the planned velocities satisfy the tangential acceleration and velocity constraints, verifying the feasibility of the occupying trajectories.

To validate the real-time performance and rapidity of the algorithm, simulations were conducted on a PC with a 3.2 GHz i3 processor and 2 GB of RAM. For 50 randomly generated sets of start and end poses, the average planning time for occupying trajectories was 0.621 milliseconds, meeting the real-time requirement.

The theoretical reasons why the algorithm satisfies real-time performance are mainly as follows: (1) The Dubins curve solution based on the discriminant table method omits the step of calculating each type of Dubins curve compared to traditional computational methods. (2) Since the parameters of the velocity curve are directly computed, the velocity curve can also be calculated in real time. For the above 50 sets of simulations, the average time for velocity planning was 28.6 microseconds, demonstrating feasibility for engineering applications.

## 5. Conclusion

This paper studies a trajectory planning method for the occupying phase of USV cooperative operations, selecting Dubins curves as the basis for occupying trajectory planning and proposing a multi-USV cooperative occupying trajectory planning algorithm based on Dubins curves. By establishing a Dubins kinematic model for USV, dynamic constraints are considered, including turning radius constraints, tangential acceleration constraints, and available velocity constraints. For the problem of solving single-USV occupying trajectory, a discriminant table is used instead of traditional geometric methods to shorten the planning time for single-USV occupying trajectory. Aiming at the operational requirement of multiple USVs reaching occupation positions simultaneously, a time coordination method for occupying trajectories is studied. Finally, simulation experiments verify the effectiveness and real-time performance of the proposed cooperative occupying trajectory planning algorithm. The results show that the proposed trajectory planning algorithm can meet the pose and time requirements for USVs to reach occupation positions simultaneously during cooperative operations, with fast computation speed.

## References

[1] Cai Qing, Sun Shiping. Research on the Characteristics and Development of Autonomous Decision-making Technology for Unmanned Surface Vessels. Ship Science and Technology, 2025, 47(05): 8-15.

[2] Lou Jiankun, Xu Mengyuan, Yue Lin, et al. Progress and Frontiers of Intelligent Navigation Technology for Unmanned

Ships. Chinese Journal of Ship Research, 2025, 20(01): 3-14.
[3] Cheng Yu, Fu Yuewen, Li Lu. Research on Simulation System of Autonomous Navigation Control for Unmanned Surface Vessels. Fire Control & Command Control, 2024, 49(01): 63-72.
[4] Sun Haiwen, Xiao Yujie, Wang Shengyu. Trajectory Planning of USV Based on Improved A* - Ant Colony Hybrid Algorithm. Ship Science and Technology, 2021, 43(15): 83-87.
[5] Wu Shanping, Huang Yanyan, Chen Tiande. Static Route Planning for Surface Ships Based on Improved A* Algorithm. Computer Engineering and Applications, 2022, 58(23): 307-315.
[6] Ning Xinjie, Cui Wei, Xu Zhaoxiang, et al. Improved Probabilistic Roadmap Algorithm. Computer Engineering and Design, 2021, 42 (12): 3422-3427. DOI: 10.16208/j. issn1000-7024.2021.12.017.
[7] Shi Yan, Zhang Lihua, Dong Shouquan, et al. Route Planning Algorithm for Anti-Ship Missiles Based on Region Division. Systems Engineering and Electronics, 2019, 41(03): 571-578.
[8] Z. Dong, R. Zhang, Z. Chen, R. Zhou, Study on uav path planning approach based on fuzzy virtual force, Chinese Journal of Aeronautics 23 (3) (2010) 341–350.
[9] Qingtian H. Research on cooperate search path planning of multiple UAVs using Dubins curve[C]//2021 IEEE International Conference on Power Electronics, Computer Applications (ICPECA). IEEE, 2021: 584-588.
[10] Dubins L E. On curves of minimal length with a constraint on average curvature, and with prescribed initial and terminal positions and tangents. American Journal of mathematics, 1957, 79(3): 497-516.
[11] Shkel A M, Lumelsky V. Classification of the Dubins set. Robotics & Autonomous Systems, 2001, 34(4):179-202.

 